SEMARAK ILMU
PUBLISHING
202103268166(003316878-P)

Semarak International Journal of
Mechanical Precision Engineering

Journal homepage:
https://semarakilmu.my/index.php/sijmpe/index
ISSN: 3083-9564

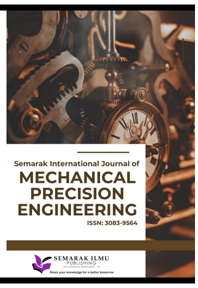

Numerical Study on Mixed Convection Stagnation-Point Flow of Reiner-Philippoff Hybrid Nanofluid Over a Shrinking Sheet

Nur Syahidah Nordin[1,2], Abdul Rahman Mohd Kasim[1,4,*], Iskandar Waini[3], Masyfu'ah Mokhtar[1,2], Siti Farah Haryatie Mohd Kanafiah[5], Imran Ullah[6]

1 Centre for Mathematical Sciences, Universiti Malaysia Pahang Al-Sultan Abdullah, Gambang, 26300 Kuantan, Pahang, Malaysia
2 Mathematical Sciences Studies, College of Computing, Informatics and Mathematics, Universiti Teknologi MARA (UiTM) Johor Branch, Segamat Campus, 85000 Segamat, Johor, Malaysia
3 Fakulti Teknologi dan Kejuruteraan Industri dan Pembuatan, Universiti Teknikal Malaysia Melaka, Hang Tuah Jaya, 76100 Durian Tunggal, Melaka, Malaysia
4 Center for Research in Advanced Fluid and Process, University Malaysia Pahang Al-Sultan Abdullah, Gambang, 26300 Kuantan, Pahang, Malaysia
5 Mathematical Sciences Studies, College of Computing, Informatics and Mathematics, Universiti Teknologi MARA (UiTM) Kelantan Branch, Machang Campus, 18500, Malaysia
6 College of Civil Engineering, National University of Sciences and Technology, Islamabad, Pakistan

ARTICLE INFO

Article history:
Received 10 December 2024
Received in revised form 17 January2025
Accepted 19 February 2025
Available online 15 March 2025

Keywords:
Reiner-Philippoff model; hybrid nanofluid; mixed convection; stagnation point; shrinking sheet

ABSTRACT

This study introduces a mathematical model that addresses the mixed convection stagnation point flow of a non-Newtonian Reiner-Philippoff hybrid nanofluid over a shrinking sheet. Through the application of theoretical assumptions, the governing equations were formulated and subsequently simplified into a set of ordinary differential equations (ODEs). The model facilitates the computation of steady flow solutions utilizing the MATLAB software function bvp4c. The primary objectives of this research include an analysis of the effects of various parameters on flow dynamics and thermal behaviour. These parameters encompass the mixed convection parameter, the solid volume fraction of nanoparticles, and the mass flux parameter, all of which significantly influence flow characteristics. Numerical results have been obtained for critical metrics, including the skin friction coefficient, local Nusselt number, and the velocity and temperature profiles. The findings contribute to a deeper understanding of hybrid nanofluid behaviour in thermal management applications, offering valuable insights for future research endeavours in the domains of fluid dynamics and heat transfer.

1. Introduction

In today's landscape, the relevance and effectiveness of non-Newtonian fluids have become increasingly significant, even though many applications still rely on Newtonian fluids, such as pure water, for cooling purposes. Advanced technologies and industrial processes require practical working fluids that can efficiently manage operations while ensuring high-quality end products.

* *Corresponding author.*
E-mail address: rahmanmohd@umpsa.edu.my

https://doi.org/10.37934/sijmpe.2.1.2436a

Numerous non-Newtonian fluids exist, each with distinct properties, and they are primarily classified based on their shear-thinning (pseudoplastic) or shear-thickening (dilatant) characteristics. Shear-thinning fluids behave similarly to Newtonian fluids at high shear rates, whereas shear-thickening fluids exhibit viscosity that rises with increasing shear rate. As noted by Deshpande *et al.,* [1], fluid models that demonstrate both shear-thickening and shear-thinning behaviours include the Reiner-Philippoff (R-P) model, Sisko model, Powell-Eyring model, Carreau-Yasuda model, and Carreau viscosity model.

The Reiner-Philippoff (R-P) model demonstrates non-Newtonian behavior at specific shear stress levels, reverting to its original characteristics when subjected to low or high shear stress. This property renders the R-P model highly significant in engineering applications and has garnered extensive attention from various scholars [2-10]. Additionally, the R-P model plays a vital role in industrial settings by accurately representing natural fluids. Under particular conditions, it can exhibit three types of fluid behavior: dilatant, pseudoplastic, and Newtonian. Understanding these behaviors is crucial for manufacturing processes, as the characteristics of the fluid in use may shift during certain procedures. Consequently, numerous studies have investigated how fluid flow interacts with different geometries and the impact of the interactions on the flow field, as can be seen in the previous study [11-18].

Modern hybrid nanofluids are increasingly utilized across various technologies to enhance thermal performance. Groundbreaking research conducted by Turcu *et al.,* [19] and subsequently by Jana *et al.,* [20] has demonstrated that the combination of different types of nanoparticles in a hybrid nanofluid yields synergistic effects, resulting in a significant increase in heat transfer rates and optimal performance. As a result, the integration of these nanofluids in industrial applications can provide substantial benefits in achieving superior thermal efficiency.

Heat transfer between different mediums occurs through moving fluids, a phenomenon known as convection. Mixed convection arises when the processes of free and forced convection are combined. The examination of mixed convection flow captures the attention of researchers due to its critical relevance in various industrial applications, such as electronic devices, heat exchangers, nuclear reactors, and solar collectors. A pivotal study conducted by Subhashini *et al.,* [21] investigated the mixed convection of nanofluid flow near the stagnation point over an exponentially stretching and shrinking sheet. The researchers considered three types of nanoparticles: copper (Cu), alumina oxide (Al_2O_3), and titanium oxide (TiO_2), using water as the base fluid. In a similar vein, Ghalambaz *et al.,* [22] examined the mixed convection at the stagnation point of hybrid Al_2O_3-Cu/water nanofluid over a vertical plate, including a stability analysis. Subsequently, Jamaludin *et al.,* [23] expanded upon the work of Subhashini *et al.,* [21] by exploring the effects of suction, thermal radiation, and heat sources/sinks in the context of a vertical stretching/shrinking sheet. More recently, Khashiie *et al.,* [24], Zainal *et al.,* [25], and Bakar *et al.,* [26] have similarly investigated the problem of mixed convection in stagnation-point boundary layer flow within hybrid nanofluids, each under varying physical conditions.

This research draws inspiration from existing literature and introduces a novel examination of the Reiner-Philippoff (R-P) hybrid nanofluid within the mixed convection stagnation point flow framework. This approach is based on a prior study that utilized the distinct R-P fluid model. The current study focuses on the flow over a shrinking sheet, aiming to optimise and enhance heat transfer for practical fluid applications. To support these goals, we developed a model that incorporates graphene oxide (GO) and molybdenum disulfide (MoS_2) nanoparticles suspended in water (H_2O) to enhance thermal conductivity. The governing equations of the model are converted into ordinary differential equations (ODEs) and solved using the bvp4c function. The computational results are presented graphically, accompanied by a detailed analysis of how various parameters impact the outcomes. Notably, our model demonstrates characteristics akin to Newtonian fluids under specific conditions, which adds to its credibility. Furthermore, the study explores the effects of mixed convection, providing a more nuanced understanding of the dynamics related to advanced applications. This model effectively addresses the complexities of fluids pertinent to real-world scenarios, making it a valuable resource for engineers and researchers alike. In conclusion, this research enhances the understanding of phenomena in advanced applications and underscores the model's relevance in optimizing and improving heat transfer in complex fluids, thereby highlighting its significance for professionals in the field.

2. Methodology

This study considers the two-dimensional steady mixed convection of R-P hybrid nanofluid flow near the stagnation point over a vertical shrinking sheet with the velocity $u_w(x) = bx^{1/3}$and the free stream velocity $u_e(x) = ax^{1/3}$, as illustrated in Figure 1. Here, $v_w(x)$ is the mass flux velocity representing the surface permeability and the surface temperature, $T_w = T_\infty + T_0 x^{-1/3}$. Besides the ambient temperature and the reference temperature, T_∞ and T_0 , respectively, are assumed to be constant. Hence, the governing equations are as follows [5,10,23]:

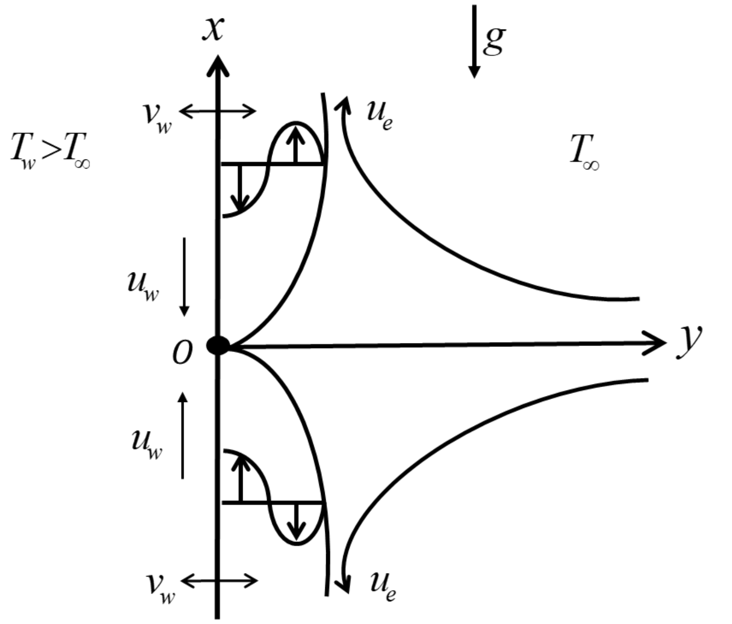

Fig. 1. The physical flow configuration model

$$\frac{\partial u}{\partial x} + \frac{\partial v}{\partial y} = 0 \tag{1}$$

$$\frac{\partial u}{\partial y} = \frac{\tau}{\mu_\infty + \dfrac{\mu_{hnf} - \mu_\infty}{1 + \left(\dfrac{\tau}{\tau_s}\right)^2}} \tag{2}$$

$$u\frac{\partial u}{\partial x}+v\frac{\partial u}{\partial y}=u_e\frac{du_e}{dx}+\frac{1}{\rho_{hnf}}\frac{\partial \tau}{\partial y}+\frac{(\rho\beta)_{hnf}}{\rho_{hnf}}g^*\left(T-T_\infty\right) \tag{3}$$

$$u\frac{\partial T}{\partial x}+v\frac{\partial T}{\partial y}=\frac{k_{hnf}}{\left(\rho C_p\right)_{hnf}}\frac{\partial^2 T}{\partial^2 y} \tag{4}$$

subject to:

$$u=u_w(x),\ v=v_w(x),\ T=T_w \text{ at } y=0$$
$$u\to u_e(x),\ T\to T_\infty \text{ as } y\to\infty \tag{5}$$

where, μ_∞ is limiting dynamic viscosity, μ_{hnf} is dynamic viscosity, ρ_{hnf} , $(\rho\beta)_{hnf}$, $\left(\rho C_p\right)_{hnf}$, and k_{hnf}, are fluid density, thermal expansion, heat capacity, and thermal conductivity, respectively. Meanwhile, *T*, $g*$, τ, and τ_s are referring to temperature, acceleration due to gravity, shear stress of R-P fluid, and reference shear stress, respectively. In addition, (u,v) are the components of velocity in the (x,y) directions. Meanwhile, the subscripts *hnf* and *f* represent the hybrid nanofluid and fluid. Employing similarity transformation as [27]:

$$\psi=\sqrt{a\nu_f}\,x^{2/3}f(\eta),\tau=\rho_f\sqrt{a^3\nu_f}\,g(\eta),\theta(\eta)=\frac{T-T_\infty}{T_w-T_\infty},\eta=\frac{y}{x^{1/3}}\sqrt{\frac{a}{\nu_f}} \tag{6}$$

The term ψ is the stream function and defined by $u=\partial\psi/\partial y$ and $v=-\partial\psi/\partial x$. Then:

$$u=ax^{1/3}f'(\eta),v=-\sqrt{a\nu_f}\,x^{-1/3}\left(\frac{2}{3}f(\eta)-\frac{1}{3}\eta f'(\eta)\right) \tag{7}$$

At $\eta=0$,

$$v_w(x)=-\frac{2}{3}\sqrt{a\nu_f}\,x^{-1/3}S \tag{8}$$

Values *S* = 0 indicates an impermeable surface, *S* < 0 indicates injection, and *S* > 0 indicates suction. Meanwhile, $\upsilon_f=\mu_\infty/\rho_f$ is the fluid kinematic viscosity.

Employing Eq. (6) and (7) obtained;

$$g=f''\left(\frac{g^2+\left(\frac{\mu_{hnf}}{\mu_f}\right)\lambda\gamma^2}{g^2+\gamma^2}\right) \tag{9}$$

$$g' - \frac{\rho_{hnf}}{\rho_f}\left(\frac{1}{3}f'^2 - \frac{2}{3}ff'' - \frac{1}{3}\right) + \left[\frac{(\rho\beta)_{hnf}}{(\rho\beta)_f}\right]Z\theta = 0 \tag{10}$$

$$\frac{1}{\Pr}\left[\frac{k_{hnf}}{k_f}\right]\theta'' + \left[\frac{(\rho C_p)_{hnf}}{(\rho C_p)_f}\right]\left(\frac{1}{3}f'\theta + \frac{2}{3}f\theta'\right) = 0 \tag{11}$$

subject to:

$$f(0) = S, f'(0) = \varepsilon, \ \theta(0) = 1$$
$$f'(\eta) \to 1, \ \ \theta(\eta) \to 0 \ \text{ as } \ \eta \to \infty \tag{12}$$

The dimensionless parameters governed the system are the Prandtl number (Pr), Bingham number (γ), RP parameter (λ), and mixed convection parameter (Z), defined as follows:

$$\Pr = \frac{(\mu C_p)_f}{k_f}, \gamma = \frac{\tau_s}{\rho_f\sqrt{a^3\nu_f}}, \lambda = \frac{\mu_f}{\mu_\infty}, Z = \frac{Gr_x}{\mathrm{Re}_x^2} = \frac{g^*(\beta)_f T_0}{a^2} \tag{13}$$

where the Grashof number is $Gr_x = \left(g^*(\beta_T)_f\left(T_0 x^{-1/3}\right)x^3\right)/v_f^2$. The value λ = 1 indicates the viscous type, λ < 1 for shear thickening and λ > 1 is shear thinning fluid. Further, the static, stretching, and shrinking sheets are denoted by ε= 0, ε> 0, and ε< 0, respectively. The physical quantities C_f and Nu_x, are given by;

$$C_f = \frac{\tau_w}{\rho_f u_w^2}, Nu_x = \frac{xq_w}{k_f(T_w - T_\infty)} \tag{14}$$

with:

$$\tau_w = \rho_f\sqrt{a^3\nu_f}\left(g(\eta)\right)_{y=0}, q_w = -k_{hnf}\left.\left(\frac{\partial T}{\partial y}\right)\right|_{y=0} \tag{15}$$

where, τ_w is the quantity of τ on y = 0, and q_w is the surface heat flux. After applying Eq. (14) and Eq. (15), one gets:

$$\mathrm{Re}_x^{1/2} C_f = g(0), \mathrm{Re}_x^{-1/2} Nu_x = -\frac{k_{hnf}}{k_f}\theta'(0) \tag{16}$$

and $Re_x = u_w(x)x/v_f$ is the local Reynolds number.

In this study, various key parameters have been carefully defined to guide the research. The Prandtl number (Pr), a dimensionless quantity that characterizes the ratio of momentum diffusivity to thermal diffusivity, is set at 6.2. This indicates a significant influence of viscous forces in the fluid.

The shrinking parameter, denoted as ε, is fixed at -1, which suggests that the fluid domain is contracting over time. Meanwhile, the Bingham number (γ), set at 0.1, reflects the fluid's yield stress characteristics, indicating a relatively low yield stress in relation to the viscous forces. The suction parameter (S), valued at 1.5, represents the intensity of the suction effect applied to the flow, while the mixed convection parameter (Z), set at -1, indicates the significance of both forced and natural convection in the system. Lastly, the R-P parameter (λ) is set to 1.5, further influencing the flow dynamics in the study. These parameters establish a comprehensive framework for understanding the fluid behaviour under investigation.

In addition, Table 1 lists the physical properties of pure water (H_2O), graphene oxide (GO), and molybdenum disulfide (MoS_2), whereas Table 2 lists the thermophysical characteristics of hybrid nanofluid.

Table 1
Thermophysical properties of H_2O, GO and MoS_2 [39,40]

Thermophysical properties	H_2O	GO	MoS_2
$\rho\left(kg/m^3\right)$	997.1	1800	5060
$C_p\left(J/kgK\right)$	4179	717	397.21
$k\left(W/mK\right)$	0.613	5000	904.4
$\beta\times10^{-5}\left(1/K\right)$	21	0.284	2.8424
Pr	6.2	-	-

Table 2
Thermophysical properties of hybrid nanofluid [28,29]

Thermophysical properties	Hybrid nanofluid
Density	$\rho_{hnf}=\left(1-\phi_{hnf}\right)\rho_f+\phi_{GO}\rho_{GO}+\phi_{MoS_2}\rho_{MoS_2}$
Heat capacity	$\left(\rho C_p\right)_{hnf}=\left(\rho C_p\right)_f\left(1-\phi_{hnf}\right)+\phi_{GO}\left(\rho C_p\right)_{GO}+\phi_{MoS_2}\left(\rho C_p\right)_{MoS_2}$
Dynamic viscosity	$\mu_{hnf}=\dfrac{\mu_f}{\left(1-\left(\phi_{GO}+\phi_{MoS_2}\right)\right)^{2.5}}$
Thermal conductivity	$\dfrac{k_{hnf}}{k_f}=\dfrac{2k_f+\dfrac{\left(\phi_{GO}k_{GO}+\phi_{MoS_2}k_{MoS_2}\right)}{\phi_{hnf}}+2\left(\phi_{GO}k_{GO}+\phi_{MoS_2}k_{MoS_2}\right)-2k_f\phi_{hnf}}{2k_f+\dfrac{\left(\phi_{GO}k_{GO}+\phi_{MoS_2}k_{MoS_2}\right)}{\phi_{hnf}}-\left(\phi_{GO}k_{GO}+\phi_{MoS_2}k_{MoS_2}\right)+k_f\phi_{hnf}}$
Thermal expansion	$\left(\rho\beta\right)_{hnf}=\left(\rho\beta\right)_f\left(1-\phi_{hnf}\right)+\phi_{GO}\left(\rho\beta\right)_{GO}+\phi_{MoS_2}\left(\rho\beta\right)_{MoS_2}$ where $\phi_{hnf}=\phi_{GO}+\phi_{MoS_2}$

3. Results

The research conducted in this study was carried out with extreme care and precision. Specific values for various parameters, including the volume fraction of nanoparticles φ, were selected to create a set of nonlinear ODEs (Eq. (9)-(11)). The obtained model is solved using a bvp4c solver. However, before solving the boundary value problems, they must first be converted into a system of first-order ODEs.

Adjusting the step size and providing an initial guess at the initial mesh point are important to achieving accurate solutions. The appropriate initial guess and boundary layer thickness are contingent upon the specific parameter values, which will help determine the solution's behaviour.

Before discussing the results in detail, it is important to note the fixed values of the influential parameters in the simulations. The range of φ values is between 0 and 0.04, where $\varphi_1 = \varphi_2 = 0$ indicates regular base fluid. The Prandtl number is set to 6.2, the shrinking parameter ε = -1, the Bingham number γ = 0.1, the suction parameter S = 1.5, the mixed convection parameter Z = -1, and the R-P parameter λ = 1.5. It should be noted that, in this study, the results are primarily focused on the case of pseudoplastic fluid (λ > 1) as compared to the other two instances of dilatant (λ < 1) and Newtonian fluid (λ = 1).

The validity of the current model is reinforced through a comparison with the theoretical predictions of $Re_x^{1/2} C_f$ provided by Yam *et al.,* [4] Given that the equations of the existing model for the limiting situation are identical, it is fitting to directly compare the current findings with these predictions. Figure 2 showcases the comparison of skin friction coefficient values against the R-P parameter (λ) for two distinct values of ε. The results are in strong alignment with those reported by Yam *et al.,* [4], highlighting an excellent degree of agreement and reliability. Furthermore, Table 3 presents numerical data that further substantiates the current model in relation to specific limiting cases.

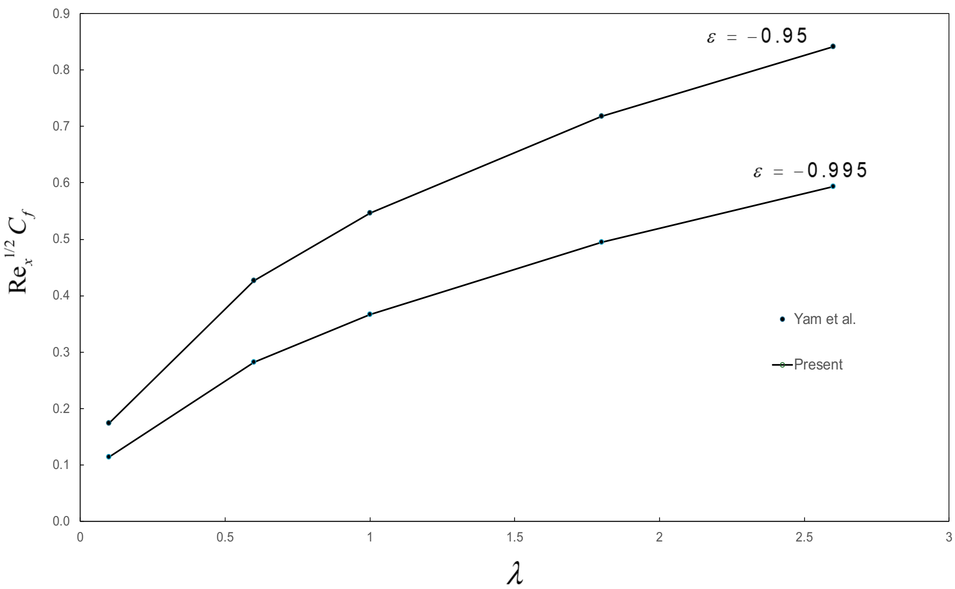

Fig. 2. Graphical comparison of the $\mathrm{Re}_x^{1/2} C_f$ against λ

Table 3
Comparative value of $\mathrm{Re}_x^{1/2} C_f$ when $S = M = \phi_{hnf} = 0$, γ = 1 and Pr = 10

λ	ε = -0.95		ε = -0.995	
	Yam et al., [4]	Present result	Yam et al. [4]	Present result
0.1	0.1740	0.174047	0.1138	0.113773
0.6	0.4264	0.426436	0.2825	0.282518
1.0	0.5470	0.546695	0.3672	0.367217
1.8	0.7175	0.717538	0.4953	0.495285
2.6	0.8412	0.841255	0.5940	0.594053

The impact of the solid volume fraction of nanoparticles (*φ*2) on $Re_x^{1/2}C_f$ and $Re_x^{-1/2}Nu_x$ are illustrated in Figures 3 and 4. Figure 3 demonstrates that the $Re_x^{1/2}C_f$ increases progressively as the value of φ rises. Brinkman [13] explained that an increase in the nanoparticle volume fraction results in higher fluid viscosity, which in turn contributes to greater skin friction along the surface. Conversely, Figure 4 indicates that as the volume fraction of nanoparticles increases, there is a corresponding decrease in $Re_x^{-1/2}Nu_x$. This phenomenon occurs because nanoparticles enhance the nanofluid's viscosity, density, and conductivity. However, this may also reduce the nanofluid's heat capacitance. Thus, there is a trade-off between the improved properties, such as heightened viscosity and conductivity and the potential decrease in heat capacitance, which can impact the overall heat transfer coefficient.

Figure 5 demonstrates the impact of suction on the reduced skin friction coefficient. Notably, the values of $Re_x^{1/2}C_f$ increase with the level of suction. This phenomenon occurs because suction at the boundary reduces the motion of the nanofluid and intensifies the velocity gradient at the surface. Figure 6 reveals that the values of $Re_x^{-1/2}Nu_x$ indicating that the heat transfer rate at the surface also rises with increased suction. Specifically, a higher magnitude of the suction parameter correlates with an enhanced heat transfer rate. This can be attributed to the fact that greater suction decreases the thickness of the thermal boundary layer, thereby increasing the temperature gradient at the surface.

The velocity and temperature profiles of the hybrid nanofluid with varying volume fractions of nanoparticles (φ_2) are illustrated in Figures 7 and 8. The analysis reveals that an increase in φ_2 results in enhanced fluid velocity. Although this rise in φ_2 is expected to elevate the fluid's viscosity, as indicated by Brinkman [13], it simultaneously increases the skin friction along the permeable vertical shrinking flat plate. This relationship is evident in the velocity profiles presented in Figure 7, where a higher φ_2 corresponds to a reduction in the momentum boundary layer thickness. Moreover, Figure 8 demonstrates that the temperature of the fluid increases with an increase in φ_2, suggesting that the temperature of the nanofluids can be effectively regulated by adjusting the volume fraction of the nanoparticles within the base fluid.

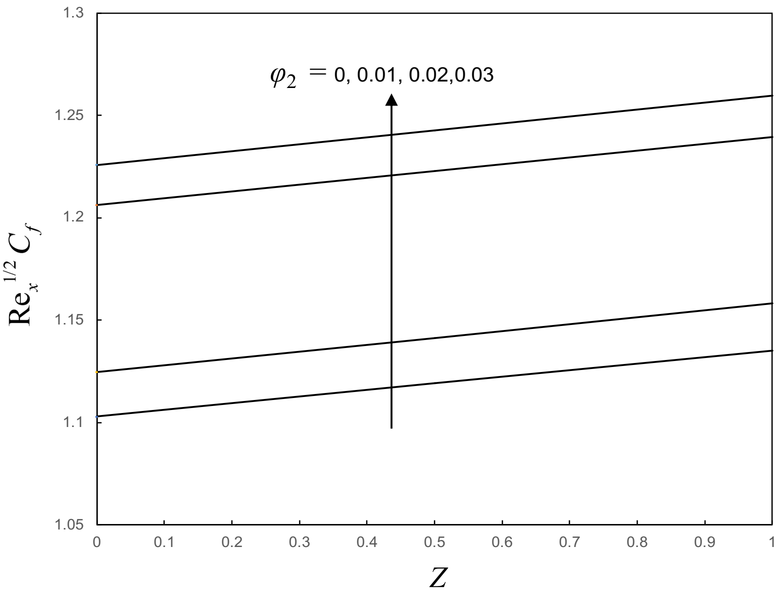

Fig. 3. $Re_x^{1/2}C_f$ vs Z for numerous values of φ_2 when Pr=6.2, the R-P parameter λ = 1.5, the shrinking parameter ε = -1, the Bingham number γ = 0.1, and the suction parameter S = 1.5

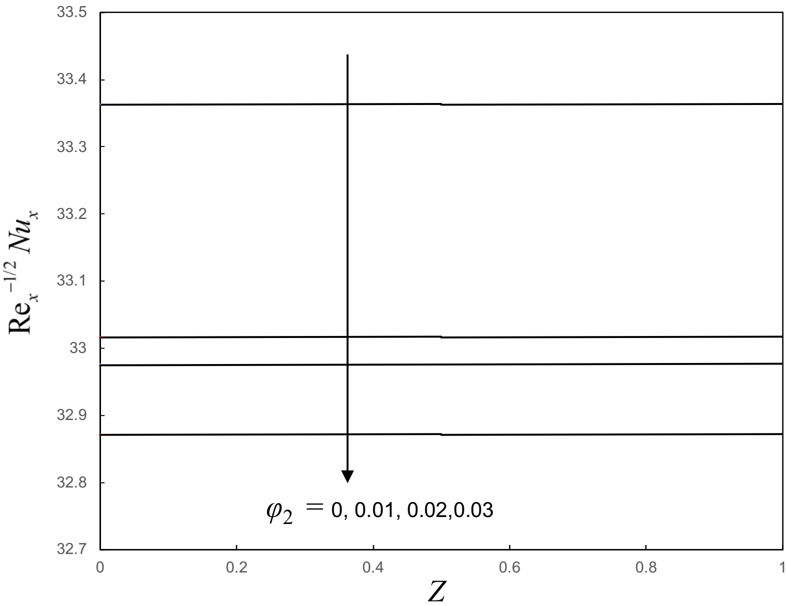

Fig. 4. $Re_x^{-1/2}Nu_x$ vs Z for numerous values of φ_2 when Pr=6.2, the R-P parameter λ = 1.5, the shrinking parameter ε = -1, the Bingham number γ = 0.1, and the suction parameter S = 1.5

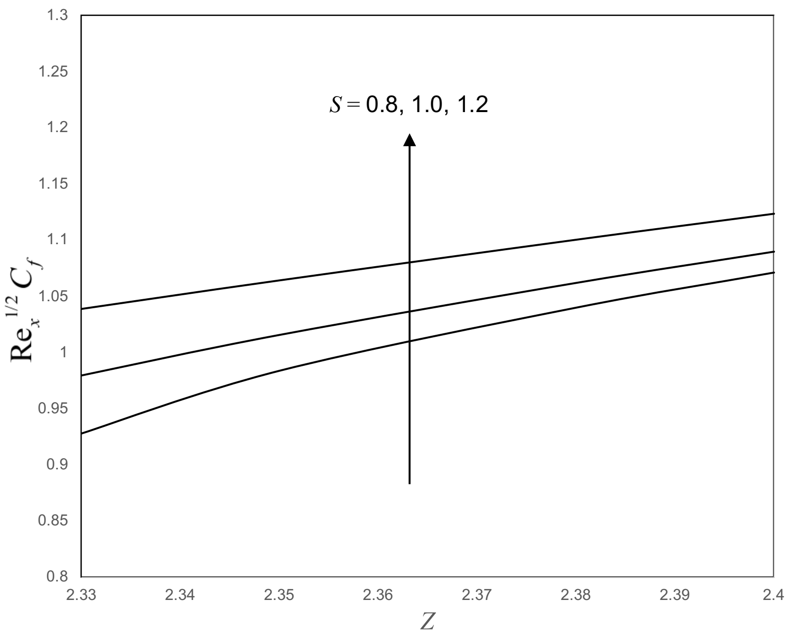

Fig. 5. $Re_x^{1/2}C_f$ vs Z for numerous values of S when Pr=6.2, the R-P parameter λ = 1.5, the shrinking parameter ε = -1, the Bingham number γ = 0.1, and the volume concentration φ_{hnf}= 0.02

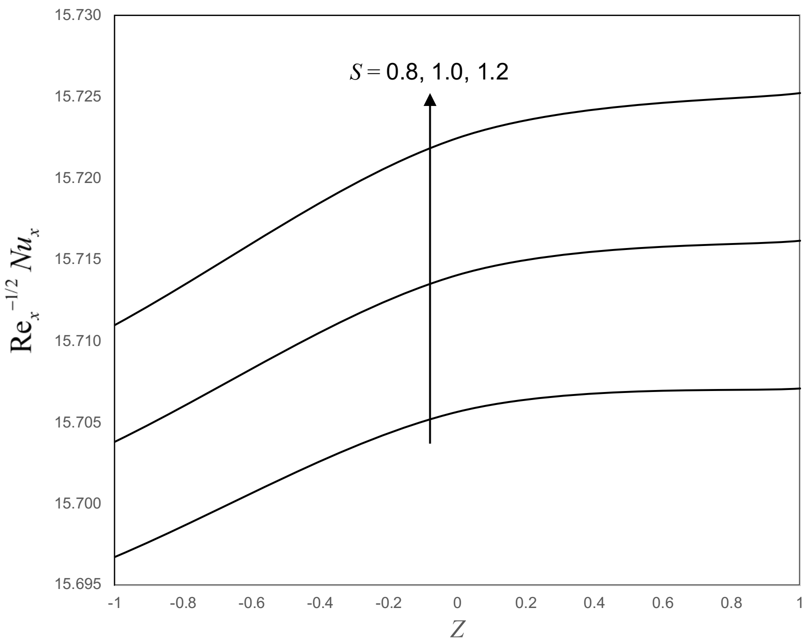

Fig. 6. $Re_x^{-1/2}Nu_x$ vs Z for numerous values of S when Pr=6.2, the R-P parameter λ = 1.5, the shrinking parameter ε = -1, the Bingham number γ = 0.1, and the volume concentration φ_{hnf}= 0.02

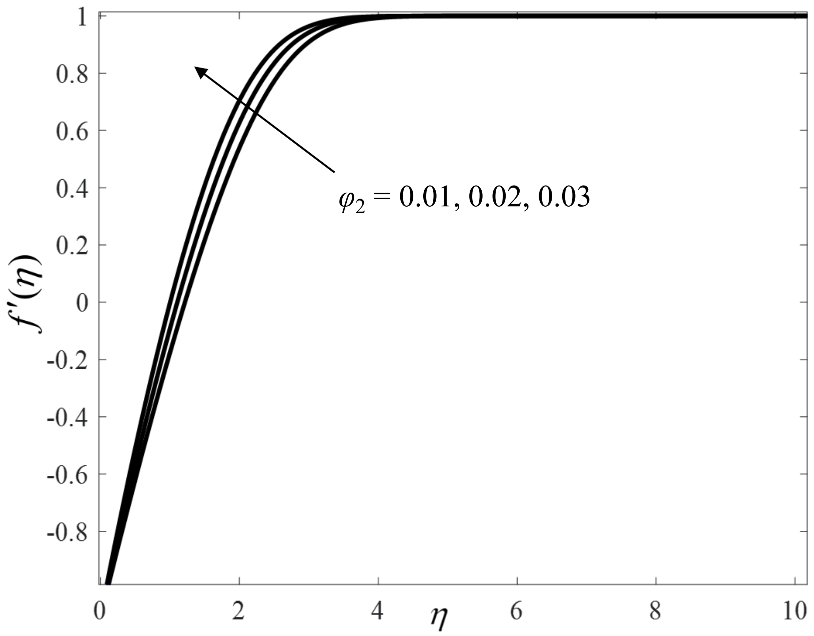

Fig. 7. The velocity profile $f'(\eta)$ for several values of φ_2 when Pr=6.2, the R-P parameter λ = 1.5, the shrinking parameter ε = -1, the Bingham number γ = 0.1, the mixed parameter Z = -0.1 and the suction parameter S = 1.5

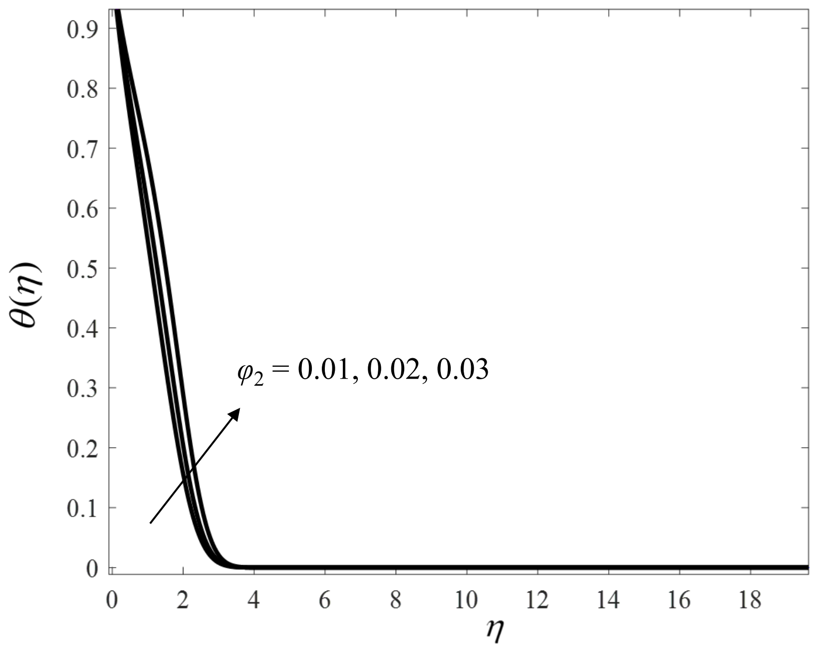

Fig. 8. The temperature profile $\theta(\eta)$ for several values of φ_2 when Pr=6.2, the R-P parameter λ = 1.5, the shrinking parameter ε = -1, the Bingham number γ = 0.1, the mixed parameter Z = -0.1 and the suction parameter S = 1.5

4. Conclusions

This study explores the mixed convection of R-P hybrid nanofluid flow near a stagnation point over a shrinking sheet. Utilizing similarity transformations and numerical methods, the researchers investigated the influence of various factors—including nanoparticle concentration, mass flux parameters, and fluid properties—on fluid flow and heat transfer. The results yield valuable insights into the potential applications of hybrid nanofluids.

i) The increase in the nanoparticle volume fraction within the nanofluid enhances the velocity distribution, temperature distribution, and skin friction coefficient. Conversely, this increment decreases the heat transfer rate at the surface.

ii) An increase in the intensity of the suction parameter S increases the values of $Re_x^{\frac{1}{2}}C_f$ and $Re_x^{-\frac{1}{2}}Nu_x$.

Acknowledgement
The authors express gratitude to Universiti Malaysia Pahang Al-Sultan Abdullah for the financial support provided through research grant PGRS2303144. We also thank Universiti Teknologi MARA (UiTM) Johor Branches, Universiti Teknologi MARA (UiTM) Kelantan Branches, National University of Sciences and Technology, Islamabad, Pakistan and Universiti Teknikal Malaysia Melaka for their valuable guidance and support.

References
[1] Abhijit P. Deshpande, Krishnan, J. Murali, and PB Sunil Kumar, eds. *Rheology of complex fluids*. New York: Springer, 2010. https://doi:10.1007/978-1-4419-6494-6

[2] Kapur, J. N., and R. C. Gupta. "Two-dimensional flow of Reiner-Philippoff fluids in the inlet length of a straight channel." *Applied Scientific Research, Section A* 14 (1965): 13-24. https://doi:10.1007/BF00382227

[3] Na, Tsung-Yen. "Boundary layer flow of Reiner-Philippoff fluids." *International journal of non-linear mechanics* 29, no. 6 (1994): 871-877. https://doi:10.1016/0020-7462(94)90059-0

[4] Yam, K. S., S. D. Harris, D. B. Ingham, and I. Pop. "Boundary-layer flow of Reiner–Philippoff fluids past a stretching wedge." *International Journal of Non-Linear Mechanics* 44, no. 10 (2009): 1056-1062. https://doi:10.1016/j.ijnonlinmec.2009.08.006

[5] Ahmad, A., M. Qasim, and S. Ahmed. "Flow of Reiner–Philippoff fluid over a stretching sheet with variable thickness." *Journal of the Brazilian Society of Mechanical Sciences and Engineering* 39 (2017): 4469-4473. https://doi:10.1007/s40430-017-0840-7

[6] Nordin, N.S., AL-Sharifi, H.A.M., Kasim, A.R.M, Waini, I., Mokhtar, M., Romlie, M.F., Samsudin, D., and Adytia, D. "Mathematical Model of Reiner-Philippoff Embedded with Al_2O_3 and Cu Particles over a Shrinking Sheet with Mixed Convection and Mass Flux Effect." *Journal of Advanced Research in Fluid Mechanics and Thermal Sciences* 111, no. 2 (2023) 195-213. https://doi.org/10.37934/arfmts.111.2.195213

[7] Khashi'ie, Najiyah Safwa, Iskandar Waini, Abdul Rahman Mohd Kasim, Nurul Amira Zainal, Anuar Ishak, and Ioan Pop. "Magnetohydrodynamic and viscous dissipation effects on radiative heat transfer of non-Newtonian fluid flow past a nonlinearly shrinking sheet: Reiner–Philippoff model." *Alexandria Engineering Journal* 61, no. 10 (2022): 7605-7617. https://doi.org/10.1016/j.aej.2022.01.014

[8] Kumar, K. Ganesh, M. Gnaneswara Reddy, M. V. V. N. L. Sudharani, S. A. Shehzad, and Ali J. Chamkha. "Cattaneo–Christov heat diffusion phenomenon in Reiner–Philippoff fluid through a transverse magnetic field." *Physica A: Statistical Mechanics and its Applications* 541 (2020): 123330. https://doi:10.1016/j.physa.2019.123330

[9] Sajid, T., M. Sagheer, and S. Hussain. "Impact of temperature-dependent heat source/sink and variable species diffusivity on radiative Reiner–Philippoff fluid." *Mathematical Problems in Engineering* 2020 (2020). https://doi:10.1155/2020/9701860

[10] Umair Khan, Aurang Zaib, Anuar Ishak, Iskandar Waini, El-Sayed M. Sherif, and Ioan Pop. "Forced convective MHD flow of Reiner-Philippoff fluid induced by hybrid nanofluid past a nonlinear moving sheet with nonlinear heat sink/source." *Waves in Random and Complex Media,* (2022): 1 – 21. https://doi.org/10.1080/17455030.2022.2070686

[11] Crane, Lawrence J. "Flow past a stretching plate." *Zeitschrift für angewandte Mathematik und Physik ZAMP* 21 (1970): 645-647. https://doi:10.1007/BF01587695

[12] Elbashbeshy, E.M.A. "Heat transfer over an exponentially stretching continuous surface with suction". *Arch. Mech.* 53 (2001) 643‑651.

[13] Brinkman, H.C. "The viscosity of concentrated suspensions and solutions". *J. Chem. Phys* 20 (1952) 571, https://doi.org/10.1063/1.1700493

[14] Zainal, Nurul Amira, Roslinda Nazar, Kohilavani Naganthran, and Ioan Pop. "Stability analysis of MHD hybrid nanofluid flow over a stretching/shrinking sheet with quadratic velocity." *Alexandria Engineering Journal* 60, no. 1 (2021): 915-926. https://doi:10.1016/j.aej.2020.10.020

[15] Khashi'ie, Najiyah Safwa, Norihan Md Arifin, Natalia C. Rosca, Alin V. Rosca, and Ioan Pop. "Three-dimensional flow of radiative hybrid nanofluid past a permeable stretching/shrinking sheet with homogeneous-heterogeneous reaction." *International Journal of Numerical Methods for Heat & Fluid Flow* 32, no. 2 (2022): 568-588. https://doi:10.1108/HFF-01-2021-0017

[16] Jamaludin, Anuar, Kohilavani Naganthran, Roslinda Nazar, and Ioan Pop. "MHD mixed convection stagnation-point flow of Cu-Al2O3/water hybrid nanofluid over a permeable stretching/shrinking surface with heat source/sink." *European Journal of Mechanics-B/Fluids* 84 (2020): 71-80. https://doi:10.1016/j.euromechflu.2020.05.017

[17] Bhattacharyya, K. "Boundary layer flow and heat transfer over an exponentially shrinking sheet". *Chinese Phys. Lett.* 28 (2011), https://doi.org/10.1088/0256-307x/28/7/074701

[18] Waini, I., A. Ishak, and I. Pop. "Magnetohydrodynamic flow past a shrinking vertical sheet in a dusty hybrid nanofluid with thermal radiation." *Applied Mathematics and Mechanics* (2022): 1-14. https://doi:10.1007/s10483-022-2807-8

[19] Turcu, R., A. L. Darabont, A. Nan, N. Aldea, D. Macovei, D. Bica, L. Vekas et al. "New polypyrrole-multiwall carbon nanotubes hybrid materials." *Journal of optoelectronics and advanced materials* 8, no. 2 (2006): 643-647.

[20] Jana, Soumen, Amin Salehi-Khojin, and Wei-Hong Zhong. "Enhancement of fluid thermal conductivity by the addition of single and hybrid nano-additives." *Thermochimica acta* 462, no. 1-2 (2007): 45-55. https://doi:10.1016/j.tca.2007.06.009

[21] Subhashini, S. V., Sumathi, R., and Momoniat, E. "Dual solutions of a mixed convection flow near the stagnation point region over an exponentially stretching/shrinking sheet in nanofluids." *Meccanica* no. 49 (2014): 2467–2478.

[22] Ghalambaz, Mohammad, Natalia C. Rosca, Alin V. Rosca, and Ioan Pop. “Mixed convection and stability analysis of stagnation-point boundary layer flow and heat transfer of hybrid nanofluids over a vertical plate.” *International Journal of Numerical Methods for Heat & Fluid Flow* 30, no.7 (2020): 3737 – 3754. https//doi:10.1108/HFF-08-2019-0661

[23] Jamaludin, Anuar, Roslinda Nazar, and Ioan Pop. “Mixed Convection Stagnation-Point Flow of a Nanofluid Past a Permeable Stretching/Shrinking Sheet in the Presence of Thermal Radiation and Heat Source/Sink.” *Energies* 12, 788 (2019) 1 – 20. https//doi:10.3390/en12050788

[24] Khashiie, Najiyah Safwa, Norihan Md Arifin, Ezad Hafidzuddin, and Nadihah Wahi. “MHD Mixed Convective Stagnation Point Flow with Heat Generation Past a Shrinking Sheet.” *ASM Science Journal* 12, no.1 (2019): 71 – 81.

[25] Zainal, Nurul Amira, Roslinda Nazar, Kohilavani Naganthran, and Ioan Pop. “MHD mixed convection stagnation point flow of a hybrid nanofluid past a vertical flat plate with convective boundary condition.” *Chinese Journal of Physics* 66, (2020): 630 – 644. https://doi.org/10.1016/j.cjph.2020.03.022

[26] Abu Bakar, Shahirah, Norihan Md Arifin, and Ioan Pop. “Mixed Convection Hybrid Nanofluid Flow past a Stagnation-Point Region with Variable Viscosity and Second-Order Slip.” *Journal of Advanced Research in Micro and Nano Engineering* 12, no.1 (2023): 1-21. https://doi.org/10.37934/armne.12.1.121

[27] Ahmad, Adeel. "Flow of Reiner-Philippoff based nano-fluid past a stretching sheet." *Journal Molecular Liquids* 219 (2016): 643-646. https://doi:10.1016/j.molliq.2016.03.068

[28] Arif, Muhammad, Poom Kumam, Dolat Khan, and Wiboonsak Watthayu. "Thermal performance of GO-MoS2/engine oil as Maxwell hybrid nanofluid flow with heat transfer in oscillating vertical cylinder." *Case Studies in Thermal Engineering* 27 (2021): 101290. http://dx.doi.org/10.1016/j.csite.2021.101290

[29] Saqib, Muhammad, Ilyas Khan, Sharidan Shafie, and Ahmad Qushairi. "Recent advancement in thermophysical properties of nanofluids and hybrid nanofluids: an overview." *City Univ. Int. J. Comput. Anal* 3, no. 2 (2019): 16-25. http://dx.doi.org/10.33959/cuijca.v3i2.27